Parallaxes and Distance Estimates for Fourteen Cataclysmic Variable Stars [1]

John R. Thorstensen

Department of Physics and Astronomy
6127 Wilder Laboratory, Dartmouth College
Hanover, NH 03755-3528;
john.thorstensen@dartmouth.edu

ABSTRACT

I used the 2.4 m Hiltner telescope at MDM Observatory in an attempt to measure trigonometric parallaxes for 14 cataclysmic variable stars. Techniques are described in detail. In the best cases the parallax uncertainties are below 1 mas, and significant parallaxes are found for most of the program stars. A Bayesian method which combines the parallaxes together with proper motions and absolute magnitude constraints is developed and used to derive distance estimates and confidence intervals. The most precise distance derived here is for WZ Sge, for which I find $43.3(+1.6, -1.5)$ pc. Six Luyten Half-Second stars with previous precise parallax measurements were re-measured to test the techniques, and good agreement is found.

Subject headings: stars – individual; stars – binary; stars – variable.

1. Introduction

Cataclysmic variables (CVs) are binary stars in which a white dwarf accretes matter from a close companion, which usually resembles a lower-main-sequence star. The dwarf novae are a subclass of CVs which show distinctive outbursts, thought to result from an instability in an accretion disk about the white dwarf. The AM Herculis stars (sometimes called "polars") are another type of CV, in which the accreted material is entrained in a strong magnetic field anchored in the white dwarf, forming an accretion funnel above the magnetic poles. Warner (1995) has written an excellent monograph on CVs.

Distances for various types of CVs are fundamentally important to physical models (see, e.g., Beuermann et al. 2000), but they have not been easy to obtain (Berriman 1987). Historically, none were near enough for trigonometric parallax. Kamper (1979) published parallaxes for some of the brightest dwarf novae, but these have proven to be incorrect (Harrison et al. 1999). The *Hipparcos*

[1]Based on observations obtained at the MDM Observatory, operated by Dartmouth College, Columbia University, Ohio State University, and the University of Michigan.

satellite obtained useful parallaxes only for a handful of the apparently brightest CVs (Duerbeck 1999). Kraft & Luyten (1965) used statistical parallaxes (proper motions and radial velocities) to determine rough absolute magnitudes for dwarf novae at minimum light. When the secondary star is visible in the spectrum (which it often isn't), and the orbital period $P_{\rm orb}$, is known, it is possible to estimate a distance spectroscopically, by combining the surface brightness vs. $T_{\rm eff}$ relation with constraints on the secondary's radius from the Roche geometry. Bailey (1981) employed a variant on this method which used K-band photometry. Because K-band surface brightness depends weakly on spectral type, and at a known $P_{\rm orb}$ the Roche tightly lobe constrains the secondary's radius, the apparent K magnitude can be used to set a lower limit on a CV's distance under the assumption that *all* the K-band light arises from the secondary. Sproats, Howell, & Mason (1996), among others, employed this technique. But a lower limit is not a distance, and the complex nature of the disk's emission makes the method problematic in many cases (Berriman, Szkody, & Capps 1985). Finally, for a small number of systems distances have been derived from spectra of the exposed white dwarf during intervals of low accretion (see, e.g., Sion et al. 1995).

Only recently have a few accurate parallaxes of CVs become available from the Fine Guidance Sensor (FGS) on HST. Harrison et al. (1999), in a breakthrough paper, reported the first accurate distances for the bright dwarf novae SS Cyg, U Gem, and SS Aur, and from these found that the secondaries of these dwarf novae are somewhat too luminous for the main sequence (Harrison et al. 2000). FGS parallaxes are also available for the novalike variables RW Tri (McArthur et al. 1999) and TV Col (McArthur et al. 2001). And just as the present paper was being completed, T. Harrison kindly communicated a draft of Harrison et al. (2003a), with precise parallaxes for WZ Sge and YZ Cnc, two of the objects studied here.

Meanwhile, the precision of ground based parallaxes has advanced dramatically thanks to the advent of CCD detectors. Monet & Dahn (1983) described early CCD parallax work and showed that very high precision was possible; Monet et al. (1992) (hereafter USNO92) gave detailed descriptions of their procedures and accurate parallaxes for dozens of stars, mostly from the Luyten Half-Second (LHS) list. Many of the parallaxes in USNO92 have formal uncertainties less than 1 mas ($= 10^{-3}$ arcsec), which is not much worse than HST parallaxes. Dahn et al. (2002) give more recent results from the USNO program and discuss further refinements of their technique. Only a handful of active CCD parallax programs exist, so the present project was partly motivated by curiosity as to how accurately a non-specialist could measure parallaxes using a general-purpose telescope.

While HST parallaxes have unsurpassed precision, HST observing time is limited and relatively few objects can be observed. I therefore attempted ground-based CCD parallax determinations of a sample of cataclysmic variable stars. The sample is not meant to be complete or representative, but was selected informally on the basis of brightness, perceived likelihood of a positive result, astrophysical interest, and observational constraints. This paper describes this program as follows. Because this is a new program, sections 2 and 3 describe the observations and analysis procedures in detail. Section 4 discusses the Bayesian method used to estimate distances from the parallaxes,

proper motions, and magnitudes. Section 5 presents the results for the individual CVs. A brief discussion follows in Section 6, and Section 7 offers conclusions.

2. Observing Procedures and Data Reduction

All the observations are from the *f*7.5 focus of the Hiltner 2.4 m telescope at MDM Observatory on Kitt Peak, Arizona. A thinned SITe 2048^2 CCD yielded a scale of $0''.275$ per 24 μm pixel. The 50 mm square filter vignetted the field of view, so the images recorded were 1760^2. The same detector was used throughout the program.

Table 1 lists the targets and gives a journal of the observations. Because the telescope is 'classically' scheduled in observing runs, the observations come in short runs of a few days separated by months or years. Thus even the best-observed targets have observations at only a modest number of independent epochs. It was not practical to schedule runs to maximize the parallax displacements of individual objects.

USNO92 explain *differential color refraction* (DCR). When different spectral energy distributions are convolved with a finite passband, different effective wavelengths result, which suffer different amounts of refraction because of atmospheric dispersion. This effect was severe for USNO92 because they used a wide passband. To minimize DCR, I chose a filter approximating Kron-Cousins I, which is narrower than the USNO92 filter and farther to the red, where atmospheric dispersion is reduced. All the parallax observations were taken with this filter. Most exposures were taken within ± 1 hr of the meridian, in order to further minimize DCR effects and other problems which might arise from telescope flexure and such. Because the DCR effects were much less severe than for the USNO, some exposures from larger hour angles were included.

On the first run, the CCD was inadvertently aligned with its columns about 2.4 degrees from true north. This (mis)alignment was maintained throughout the program, with the exception of 1999 June, when the alignment was not set correctly. There was no obvious problem with the 1999 June data, so this step may not have been necessary.

When each target was first observed, it was centered approximately on the CCD and its pixel coordinates noted. For all subsequent observations, the pointing was reproduced within roughly 20 pixels in order to minimize the effects of any optical distortion and to allow use of a consistent set of reference stars.

In order to avoid saturating the reference or (sometimes) program star images, exposures were generally kept to < 100 s, reaching 25 s in some cases. Reading and preparing the CCD took more than two minutes, so efficiency suffered. Many (typically ~ 10) exposures were taken at each pointing. From time to time the telescope was 'dithered' by a few pixels between exposures in a sequence.

As one might expect, the seeing strongly affected the results. Pictures taken in poor seeing

had large fit residuals. For this reason, few data are included from images with seeing worse than 1.5 arcsec FWHM, and the majority of the data are from images with < 1 arcsec seeing. The very best images included are around 0.6 arcsec, still not quite undersampled.

When the sky was suitably cloudless, exposures in the $UBVRI$ filters (or sometimes only V and I) were added to the program, together with standard star fields from Landolt (1992) to allow transformation to standard magnitudes. Photometric exposures were obtained on at least two nights, and the results were averaged after analysis. The consistency was generally better than 0.05 mag.

The data were reduced using standard IRAF[2] routines for bias subtraction and flat field correction. The flat fields were constructed from offset, medianed images of the twilight sky.

3. Data Analysis

Star centers were measured with the IRAF implementation of DAOPHOT (originally written by Stetson 1987), which constructs a model point-spread function (PSF) from selected stars and fits these to the program stars. Because the centroid information is contained in the steep sides of the PSF, a small fitting radius was used, generally 0.8 arcsec. For some of the later measurements, the fitting radius was adapted to the seeing on the individual pictures.

The measurement procedure was automated as follows. First, the average of several of the best pictures (the 'fiducial' frame) was examined to select a set of stars to measure and a set of suitable PSF stars. Next, lists of stars on all the pictures frames were generated using *daofind* or *SExtractor* (Bertin & Arnouts 1996). A computer program matched objects on these lists to the corresponding objects on the fiducial frame, and the matches were used to transform the program and PSF star coordinates to the system of each picture. The DAOPHOT measurements proceeded automatically.

To determine the true scale and orientation of the fiducial frame, the star images were matched to the USNO A2.0 catalog (Monet et al. 1996), which is aligned with the ICRS (essentially J2000). In most fields several dozen stars were matched, with plate solutions typically having RMS residuals of $0.''3$, mostly from the centering uncertainty of the USNO A2.0 and proper motions since the USNO A2.0 plate epoch. Given the number of stars in the solutions and the size of the field, the image scales derived from these fits should be accurate to a few parts in 10^4, and the orientation should be accurate to a ~ 0.03 degree. Using the scale and orientation, the pixel coordinates of the fiducial stars were transformed to tangent plane coordinates $X_{\rm fid}$ and $Y_{\rm fid}$, with the program object at the origin. These coordinates correspond closely to $\Delta\alpha$ and $\Delta\delta$ over a small field.

Once the fiducial stars were characterized, a computer program collated the DAOPHOT im-

[2]The Image Reduction and Analysis Facility, distributed by the National Optical Astronomy Observatories.

age centers from the original pictures, and generated a master raw data file containing the fixed information about the measured stars, the celestial location, the Julian dates of the exposures, and the measured image centers $(x_{\rm DAO}, y_{\rm DAO})$ from all the pictures. In addition, a weight of zero or one was assigned to each star indicating whether it was to be used in generating coordinate transformations. The program star was never used for the coordinate transformations, and other stars were eliminated from the transformations if preliminary analysis showed large scatter or (in some cases) large proper motions or parallaxes.

The analysis proceeded in several steps as follows:

1: Computable corrections. For each star, corrections for differential refraction, differential aberration, and DCR were computed, in the $(X_{\rm fid}, Y_{\rm fid})$ system. A transformation was derived between $(x_{\rm DAO}, y_{\rm DAO})$ and $(X_{\rm fid}, Y_{\rm fid})$. The net correction was transformed back to the $(x_{\rm DAO}, y_{\rm DAO})$ system, and added to the original coordinates. Thus the coordinates were 'born corrected'. Routines adapted from *skycalc*[3] performed the spherical trigonometry calculations. Tests showed that with the exception of DCR (discussed below), these corrections generally made relatively little difference to the results, because their effects were largely absorbed by the 'plate model' later in the process.

The DCR correction calls for some discussion. Early experiments with fields deliberately taken both near and far from the meridian suggested a DCR coefficient near 7 mas per unit $(\tan z)$ per unit $(V - I)$, whereas the polynomial given by USNO92 implies a value of 29 in the same units for their broader passband. I checked the empirically-derived DCR coefficient using a procedure outlined by Gubler & Tytler (1998), as follows. Library spectra from Pickles (1998) were convolved with passbands from Bessell (1990) to compute effective wavelengths as a function of $V - I$, and a *slalib* (Wallace 1994) routine was used to to find the refraction as a function of wavelength. The final result was 5 mas per unit $(\tan z)$ per unit $(V - I)$, in reasonable agreement with the empirical 7. To verify the procedure, the calculation was repeated for the USNO92 passband (approximated as flat across their coverage), and their value of 29 units was recovered successfully.

2: Position averaging. The $(x_{\rm DAO}, y_{\rm DAO})$ coordinates were transformed to the system outlined by $(X_{\rm fid}, Y_{\rm fid})$, using a four-constant plate model (which allows only shifts in zero point, a rigid rotation, and a scale change). These positions were averaged to create refined positions $(X_{\rm fid2}, Y_{\rm fid2})$ for each star. The errors in these positions were much reduced because of averaging over many frames and because of the previous step's removal of computable offsets.

3: Iteration. The transformations between $(x_{\rm DAO}, y_{\rm DAO})$ and the XY system were computed again using $(X_{\rm fid2}, Y_{\rm fid2})$ as the target coordinates and using a more flexible plate model of the form

$$X' = a_0 + a_1 X + a_2 Y + a_3 X^2 + a_4 XY + a_5 Y^2 + a_6 X r^2 + a_7 Y r^2,$$

[3]This time-and-the-sky program was written by the author, and is available from ftp.iraf.edu in the contrib directory.

where r is the radial distance from the fiducial point at the middle of the field, and similarly for Y. This model was needed to adequately account for variable systematic distortions across the wide field of view. The $(x_{\rm DAO}, y_{\rm DAO})$ coordinates were transformed onto this system, and residuals were formed by subtracting away $(X_{\rm fid2}, Y_{\rm fid2})$. These formed the time series of offsets in X and Y to be fitted in the next step.

4: First pass fitting. The residuals of each star were fitted to

$$X(t) = X_0 + \mu_X(t - \bar{t}) + \pi p_X(t)$$

and similarly for Y, where t is the time (Julian date) and $\bar{t}$ is its mean, X_0 and Y_0 are small offsets relative to the star's adjusted fiducial position, μ_X and μ_Y are proper motions, and $p_X(t)$ and $p_Y(t)$ are the parallax factors along each axis at time t for the star's α and δ, which were computed using a *skycalc* routine. The fitting was done in a somewhat unorthodox manner; first estimates of the parameters were computed using linear least-squares fits to X and Y separately, and then a numerical steepest descent algorithm was used to minimize

$$\sum_i \left\{ [X_i - X(t)]^2 + [Y_i - Y(t)]^2 \right\},$$

where (X_i, Y_i) is the i-th data point; this explicitly couples the X and Y solutions through the common parameter π. Fig. 1 gives an example of how the residuals are fitted (though for the data shown all the iterations described below have been performed).

5: Iteration (again). The coordinate transformations were computed again, this time adjusting the stars' fiducial positions for the proper motion and parallax displacements at the epoch of each picture. In practice this made little difference, since stars with large enough motions to matter were generally eliminated from the fit earlier in the process because of their large residuals. Residuals between the stars' positions on individual frames and their mean positions were again computed and used as the basis for the final step.

6: Final fitting. The residuals were fitted again, as in step (4) above. Formal uncertainties were estimated using the procedure outlined by Cash (1979); essentially, error bars were drawn at critical levels of the mean square fit residual. This procedure assumes that the fitted parameters are uncorrelated. This is only defensible in this case if the observations extend over enough epochs to cleanly separate parallax and proper motion. The observations reported here generally satisfy this criterion.

7: Human Editing. The reduction code allows the user to examine and edit the input data; the whole process (1 – 6) can then be run again. The fit residuals from individual pictures were examined and pictures with particularly large scatter, generally due to poor seeing, were removed. The comparison star fits were reviewed individually, and objects with large scatter (due to faintness or other difficulties such as incipient duplicity) were eliminated from the reference grid. The reference stars making the final cut generally had RMS residuals below 10 mas. In some instances reference

stars were eliminated because of their large proper motions, which would skew the zero point of the proper motions.

The result of steps 1 – 7 was a set of parallaxes, proper motions, and formal errors for all the stars which had been measured in each field. Table 2 (available in full in the electronic version of this paper) presents this information, along with the celestial coordinates, V and $V-I$ magnitudes, RMS residuals of the fits, and statistical weights.

A correction to absolute parallax was estimated as follows. For each star used for the reference frame, a distance was estimated from the measured I and $V-I$ color, using typical main-sequence values tabulated by Pickles (1998). The straight mean of the estimated reference-star parallaxes was used to correct the relative parallax to absolute. Reddening of the reference stars was not taken into account, nor was the possibility that they might be giants, which we cannot exclude. At high latitudes, giants of the apparent magnitude of the reference stars would be far out in the halo and hence unlikely *a priori*; at lower latitudes, where many more reference stars were available, a few mis-identified giants would lead to a slight overestimation of the very small correction. The use of I magnitudes mitigated the effects of absorption to some extent; in any case, unaccounted-for extinction would somewhat counter-intuitively tend to make the stars appear closer than their true distances, because the reddening would make the stars appear later-type, and hence absolutely fainter, and hence closer than their true distance. The extinction would also make the stars appear fainter (and hence farther away), but the former effect more than compensates for the latter. Accordingly, this estimate is in effect an upper limit to the correction. The corrections were in all cases small, of order 1 mas, and the uncertainty in the correction was ignored.

The number of stars measured in each field was large enough to allow an alternate calculation of the parallax error, as follows. A set of stars was chosen for proximity on the sky and similarity in brightness, and the scatter of the fitted parallaxes of these stars was taken as an alternate parallax uncertainty. The magnitude and radius window was adjusted to include ~ 10 stars or more in the sample; typically stars within 3 arcmin and ± 1 mag of the program star were included, but this varied widely based on how many stars were available. The scatter was computed both around zero and around the stars' photometric parallaxes, but the photometric parallax adjustments were small enough, and the errors large enough, that this made little difference in practice. This measure of parallax uncertainty was usually somewhat greater than the fit errors above, but they were not dramatically larger, indicating that the fit errors were not too far off. Nonetheless, these measures are probably more faithful indicators of the true external error, and they were used in the distance estimates given later, except in those cases in which the estimated external error was *less* than the formal error, which could happen because of the small number of stars involved.

Error of a single measurement. The scatter around the parallax and proper motion fits for the best, stablest comparison stars is around 6 mas (vector rms error). This is about double the error obtained at USNO with a similar CCD and slightly poorer image scale (Dahn et al. 2002).

The short exposure times used in the present study may contribute to this in the following

way. The effectiveness of 'tip-tilt' adaptive optics schemes demonstrates that bulk image motion is a major contributor to seeing. Typical amplitudes of the bulk image motion are 200 mas or so. The coherence time of the atmosphere in good seeing is of order 30 milliseconds, so one obtains effectively 30 independent samples of the image motion for each second of exposure time, or 1800 such samples in a typical 60 s exposure. The image centers should therefore be displaced by approximately (200 mas) $/\sqrt{1800}$, or around 5 mas. If all the stars suffered the same displacement this would be of no concern, but the seeing only correlates over the isoplanatic patch, which is typically less than a couple of arcmin in size. Indeed, examining residual maps from individual frames in succession, there is a strong impression that residuals correlate over patches of roughly this size and vary from picture to picture.

The USNO telescope is also a purpose-built astrometric telescope, while the Hiltner telescope is not. Unmodeled optical distortions over the relatively wide field may contribute to the error budget; the fairly complicated plate model needed to adequately model the reference frame indicates that this is likely the case.

Accuracy of the Proper Motions. The formal errors in the proper motions are generally very small, of order 1 mas yr^{-1} in most cases. However, no attempt was made to put these in an absolute frame. Scatter diagrams of the proper motions in all of the fields suggest that small-number statistics typically affect the mean reference star motion at the 2 to 3 mas yr^{-1} level; as noted earlier, exceptionally high proper motion reference stars were eliminated to avoid skewing the zero point excessively. At high latitudes the reference star grids were relatively sparse and the proper motions noticeably larger than at low latitude, where more distant reference stars are available; both these effects make the proper motion zero point at high latitude somewhat more loosely defined than at low latitude. The high-latitude frames often have detectable galaxies, which could in principle constrain the zero point, but it was felt that the centroids of these extended objects could not be defined with sufficient precision to make this worthwhile.

3.1. Checks Using Nearby Stars

To check the above procedures, I re-observed several of the Luyten Half-Second (LHS) stars with precise parallaxes published by Monet et al. (1992). These were for the most part not observed as extensively as the program stars, but the agreement is nonetheless satisfactory. Because similar sets of comparison stars were used in the two determinations, the correction to absolute parallax is ignored, as it should have almost no effect on the comparison.

Table 3 lists the results. A few of these deserve comment. LHS 429 is extremely red, and hence requires a relatively large DCR correction. Turning off the DCR correction decreases $\pi_{\rm rel}$ by about 10 mas, ruining the good agreement with Monet et al. (1992), and offering a somewhat roundabout check on the DCR correction procedure. LHS 1801 and 1802 are a common proper motion pair, for which the USNO parallaxes differ by 2.5 of their mutual standard deviation; the MDM parallaxes are

internally consistent, though slightly smaller than the USNO parallax. Interestingly, there are slight but significant differences in the proper motions between the two stars which are nearly identical in the two determinations, suggesting that orbital motion is detected. Finally, a foreground L3.5 dwarf was discovered serendipitously among the stars measured in the field of LHS 1889 (Thorstensen & Kirkpatrick 2003).

4. Distance Estimation

For a uniform distribution of objects in space, the distribution of true parallaxes π is proportional to $1/\pi^4$, because the volume element at a distance $r = 1/\pi$ is proportional to $r^2\,dr$. From this, Lutz & Kelker (1973) show that if parallaxes have substantial relative uncertainties, they tend to systematically underestimate distance. If the measured parallax π_0 is assumed to have Gaussian-distributed measurement errors with standard deviation σ_π, π is distributed as

$$L(\pi|\pi_0) = \frac{e^{-(\pi-\pi_0)^2/2\sigma_\pi^2}}{\pi^4}.$$

(The vertical bar in the argument of L is read as 'given', as is standard; this is therefore 'the likelihood of π given a measurement π_0'.) This expression does not include any *a priori* constraint on the distance – the objects can be any absolute magnitude, for example. In their treatment the local maximum of L is taken as the best estimate of the true parallax. If the relative error σ_π/π_0 is small, the maximum of L lies near π_0 and the correction is fairly minor; at $\sigma_\pi/\pi_0 = 0.15$, for example, the distribution of true parallaxes resembles a Gaussian with a peak at $\pi = 0.9\pi_0$. There is always a formal singularity near $\pi = 0$, but for small relative error this occurs at distances so large as to be implausible (see Fig. 1 of Lutz & Kelker 1973) [4]. However, as the relative error increases, the singularity near $\pi = 0$ become dominant, and at $\sigma/\pi_0 = 0.25$, the local maximum in L disappears and there is no longer a unique estimate of π (Smith 1987a). In this framework, even a '4 σ' parallax detection is likely to be a near-zero parallax which has been bumped up to the observed value by observational error, because the volume of space at small parallax is so large. This difficulty at low signal-to-noise might be called the 'Lutz-Kelker catastrophe'.

Several of the stars studied here have parallaxes in the $\sim 3\sigma$ to 5σ range, significant if the Lutz-Kelker bias is *not* taken into account, but formally insignificant if the Lutz-Kelker correction is taken at face value. The formal insignificance does not seem plausible, since there is other evidence for the relative proximity of these stars, as follows. (1) In some cases the CVs have significantly larger proper motions than the reference stars. (2) The absolute magnitudes can often be constrained by other evidence, and in any case these objects cannot have the very high luminosities implied by great distances. (3) The target stars, which have been selected *a priori* as cataclysmic variables,

[4] It is interesting to note that the infinity near $\pi = 0$ is severe enough that the cumulative distribution function is undefined unless the domain of the probability distribution is restricted to be greater than some nonzero parallax.

generally have the largest parallaxes, or close to it, among all the stars measured in the field. The Lutz-Kelker catastrophe arises because of random fluctuations operating on a skewed underlying parallax population – why should the target stars be singled out?

We thus seek a way to incorporate our prior expectation that the objects are *not* at extreme distance, in order to suppress the Lutz-Kelker catastrophe. Lutz & Kelker (1973) themselves remove the formal infinity at zero parallax by arbitrarily imposing a lower limit to the parallax (their ϵ).

Bayesian probability provides a formal structure for incorporating prior information in parameter estimation (Loredo 1992) [5]. I therefore used Bayesian inference to construct an *a posteriori* probability density for the parallax, using as prior information the proper motion together with an assumed velocity distribution, and the apparent magnitudes together with a broad range of assumed absolute magnitudes. This approach is cogently detailed by Smith (1987a) and Smith (1987b). The formalism used here is nearly identical.

In order to make use of the proper motions, a distribution of velocities must be assumed. With the simplifying assumption of an isotropic velocity distribution, the γ-velocities (i.e., mean systemic radial velocities) give a measure of the transverse velocity distribution. van Paradijs, Augusteijn, & Stehle (1996) tabulated observed γ velocities from the literature and found, for non-magnetic systems, an overall dispersion of 33 km s^{-1}, without strong dependence on subtype. One might expect a subtype dependence – Kolb & Stehle (1996) predict that long-period systems should be relatively young, and hence have a low velocity dispersion, and indeed North et al. (2002) find an extremely low velocity dispersion among four systems they studied. Shorter-period systems may be more ancient, and hence have higher dispersions. In order to check this possibility with a possibly more homogeneous sample, I collected γ-velocities of systems with $P_{\rm orb} < 2$ hr from published MDM observations (Thorstensen et al. 1996; Thorstensen 1997; Thorstensen & Taylor 1997; Thorstensen et al. 2002; Thorstensen & Fenton 2003), most of which were not available to van Paradijs, Augusteijn, & Stehle (1996), and from another ten systems for which results are in preparation. All 28 stars in this sample were observed with similar spectral resolution and calibration procedures, which should minimize excess scatter. The LSR-corrected velocities had $\bar{v} = -9$ and $\sigma_v = 28$ km s^{-1} (excluding RZ Leo, which had a very poorly-measured orbit). Both this result and van Paradijs et al.'s estimate should be upper limits to σ_v, since the emission lines do not necessarily track either star closely. The velocity dispersion of the shorter period systems appears thus to be quite small, probably only just consistent with the predictions of Kolb & Stehle (1996) (their Fig. 3).

Smith (1987b) develops a formalism for computing the *a priori* likelihood of a proper motion as a function of distance, when the parent population has a triaxial Gaussian velocity distribution aligned with Galactic coordinates, with dispersions σ_U, σ_V, and σ_W in the three principal directions (his equations 25 and 26). I modified this formalism as follows. Guided by the velocity dispersion

[5] A useful expanded version of this article is available at astrosun.tn.cornell.edu/staff/loredo/bayes/tjl.html

results noted above, I assumed the bulk of the CV population to have the kinematics of Galactic K0 giants as tabulated in Mihalas & Binney (1981) (p. 423), with $(\sigma_U, \sigma_V, \sigma_W) = (31, 21, 16)$ km s^{-1}. I added to this a high-velocity tail with a normalization of 0.05 times the bulk population, with (100, 75, 50) km s^{-1}, similar to the subdwarfs. Finally, I added a lower-velocity core, with 0.2 times the normalization, with (24, 13, 10) km s^{-1}, similar to F0 dwarfs. This composite probability density was evaluated over a range of hypothetical true parallaxes. The proper motion was adjusted to the local standard of rest at each parallax before the probability density was evaluated. The uncertainty in the proper motion determination (eqn. 27 in Smith 1987b) was ignored.

The apparent magnitudes of many of these systems can also be used to constrain the distance. Warner (1987) (also Warner 1995) showed that the absolute magnitudes of dwarf novae at maximum light, corrected for inclination, are strongly correlated with $P_{\rm orb}$. For $P_{\rm orb} < 2$ hr, the maximum magnitude generally occurs in superoutburst, which is about a magnitude brighter than normal outburst; I assumed this to be the case. The optical colors of dwarf novae in outburst are fairly close to zero, so the distinction between $m_{\rm pg}$ and $m_{\rm V}$ is ignored. The orbital inclinations for most of the program objects are uncertain, so the inclination correction is not known. To account for this and unexpected scatter in the relation, and to avoid 'assuming what we are trying to prove', the magnitudes were assumed to follow a very broad Gaussian. Sometimes other constraints on the distance were available (e.g., from detections of secondary stars), and again relatively broad probability distributions were assumed to avoid steering the estimate too much. The notes on individual stars detail the adopted absolute magnitude constraints.

The parallax, proper motion, and magnitude information was combined as follows.

Bayes' theorem states, in general terms

$$P(H|DI) \propto P(D|HI)P(H|I),$$

where P represents a probability, H the hypothesis, D the data (in this case, the observed parallax), and I the prior information about the problem (constraints derived from the proper motion and magnitude, and assumptions such as the normal distribution of errors). In this case H is a hypothesized true parallax, e.g. 'VY Aqr has a true parallax of 8.2 mas', and we are asking for the likelihood that H is correct given D (the measured parallax and its estimated uncertainty) and I (the proper motion and the assumptions about the space velocity, the apparent magnitude and the assumptions about the plausible range of absolute magnitudes, and the assumed normal distribution of the experimental error). The true parallax can be any positive number, so we run the computations for a range of parallaxes from near 0 up to large values (i.e., we vary H), creating a continuous probability density. This continuous probability density for $P(H|DI)$ is exactly what we want: the relative likelihood of each *true* parallax, *given* all the information we have available, including our measurement.

The first factor on the right is the probability of obtaining our measured parallax, for the given true parallax and the prior information. Once the true parallax has been fixed, the assumption of

a normal error distribution yields

$$P(D|HI) \propto e^{-(\pi-\pi_0)^2/2\sigma_\pi^2}.$$

Since the true parallax is held fixed at an assumed value, the proper motion and magnitude constraints do not affect this factor.

The second factor is the *a priori* probability of a particular parallax, given only the prior information. This itself is composed of several factors. The proper motion probability density is included here. The magnitude constraint is somewhat more difficult, because of bias. Smith (1987b) treats the case of a Gaussian distribution of absolute magnitudes for the type in question, and formulates a Malmquist-type adjustment to the most likely absolute magnitude which accounts for the tendency to pick out absolutely brighter (hence more distant) members of a population with a non-zero luminosity dispersion. The correction replaces the mean absolute magnitude M_0 with $M^* = M_0 - 1.84\sigma_M^2$. Alternatively, one can formulate a density by simply multiplying the volume element ($\propto 1/\pi^4$) by the appropriate Gaussian weighting function centered on M_0. Somewhat counter-intuitively, these approaches give the same probability density. Because of the very broad Gaussians used to characterize the luminosity priors of most of the cataclysmics, these functions end up resembling pure $1/\pi^4$ distributions, except that the singularity as $\pi \to 0$ is eliminated by the Gaussian cutoff in absolute magnitude.

The calculation for each star proceeded as follows. The estimated $\pi_{\rm abs}$ and its external error, the estimated absolute magnitude and catalogued apparent magnitude (as appropriate for the type of CV and outburst state) were tabulated; the values used are given in Table 4 and commented on further in the notes below. A grid of 'true' parallax values π was constructed, from 0.1 to 30 mas in 0.1 mas increments. This upper limit was chosen to be safely larger than any of the measured parallaxes. At each parallax, the probability density $P(D|HI)$ was computed, and a cumulative distribution function was formed from these. The points at which the cumulative distribution equaled 0.50, 0.159, and 0.841 were taken as the best estimate of the parallax and the positive and negative '1-sigma' error bars. Fig. 1 illustrates this process for VY Aqr, and the last columns of Table 3 give the results.

5. Results

Table 4 summarizes the parallax measurements and the distances derived from them. A discussion of individual objects follows.

VY Aqr: The parallax alone, $\pi_{\rm abs} = 11.2 \pm 1.4$ mas, gives a distance near 89 pc. The relative error is small enough that the Bayesian adjustments to this are fairly minor. VY Aqr is an SU UMa star with an orbital period of 0.06309(4) d (Thorstensen & Taylor 1997). The orbital inclination is unknown, but emission lines in quiescence are strongly double-peaked, suggesting $i > 50$ degrees, and there is no hint of an eclipse, suggesting $i < 75$ degrees, so I adopt $i = 63 \pm 13$ degrees, which

combined with the orbital period yields $M_V(\max) = 5.8 \pm 0.7$ using the Warner (1987) relation. Patterson et al. (1993) studied the outbursts; they do not quote $V_{\max}$ for normal outbursts, but from their figures I estimate this to be 10.8, with an uncertainty of at least a few tenths of a magnitude. In the Bayesian calculation a generous $\sigma = \pm 3$ mag was used, effectively unweighting the magnitude constraint. The proper motion probability density peaks near $\pi = 8$ mas, corroborating the parallax. The Bayesian distance estimate, 97 (+15,−12) pc, is slightly larger than $1/\pi_{\rm abs}$, mostly because of correction for the bias. Recently, Mennickent & Diaz (2002) detected the secondary star in the infrared, and estimated a distance of 100 ±10 pc, in excellent agreement with the parallax-based estimate.

SS Aur: Harrison et al. (2000) find $\pi_{\rm rel} = 3.74 \pm 0.63$ mas from the HST FGS, and estimate $\pi_{\rm abs} = 5.22 \pm 0.64$ mas, which after a Lutz-Kelker correction yields a most probable parallax of 4.97 mas. The parallax here, $\pi_{\rm abs} = 4.8(1.1)$ mas, is not as precise but agrees nicely on the face of it.

The prior information for the distance estimate (excluding the HST FGS parallax for independence) is as follows. The secondary star in SS Aur is an M1V (Friend et al. 1990; Harrison et al. 2000), and the spectral energy distribution suggests that most of the K-band luminosity is from the secondary. A normal M1V has $M_K = +5.5$ (Beuermann et al. 1999), and Harrison et al. (2000) measure $K = 12.66$; I take this as the best prior distance estimate, and assign a ±1 mag standard deviation. For purposes of testing the Warner relation (discussed later), I adopt $V_{\max} = 10.3$ from the GCVS and take $i = 39 \pm 8$ deg from a dynamical study of the secondary by Friend et al. (1990). The MDM proper motion is small, $(\mu_\alpha, \mu_\delta) = (+1.7, -20.8)$ mas yr^{-1}, in fair agreement with the the Lick Northern Proper Motion Survey (Klemola, Jones, & Hanson 1987, hereafter NPM) which gives (+8.2, −15.3) mas yr^{-1}, with a statistical error ~ 5 mas yr^{-1}, in a frame referred to external galaxies. Harrison et al. (2000) find (+8.3, −3.4) mas/yr, which disagrees significantly in μ_δ with the Lick and MDM determinations. Two of their four reference stars are in my field, and for those two I find (−0.5, −4.9) mas yr^{-1} for their star 'SS Aur 2', and (6.4, −7.2) mas yr^{-1} for their 'SS Aur 12'. They do not comment on the proper motions of their reference stars; I therefore adopt the MDM proper motion.

The proper motion-based parallax probability density peaks near $\pi = 3$ mas, and the secondary star absolute magnitude constraint peaks just below $\pi = 4$ mas. Because of the substantial relative error of the parallax, the π^{-4} correction enters strongly, giving a final estimate of 283 $(+90, -60)$ pc. This is just consistent with the more accurate HST distance, 200 ± 30 pc, but adds little weight.

Z Cam: The orbital period of this prototypical Z Cam star is 6.98 hr (Kraft, Krzeminski, & Mumford 1969; Thorstensen & Ringwald 1995). Eclipses are not observed, but the light curve shows structure at the orbital period, indicating that the inclination is not too low. Adopting $i = 65 \pm 10$ degrees, the $M_{\max}$ - $P_{\rm orb}$ relation (Warner 1987) gives approximately $M_V \sim +4.3(+0.6, -0.9)$, which combines with $V_{\max} = +10.4$ (estimated from Oppenheimer, Kenyon, & Mattei 1998) to yield a most likely $m - M = +6.1$, or $d = 165$ pc. Szkody & Wade (1981) classify the secondary

star as K7 and, assuming it is somewhat larger than the ZAMS at that type, place the star at 200 pc, or $m-M=+6.5$. Based on these I conservatively adopt a prior estimate of $m-M=6.2\pm1.5$. The MDM proper motion is $(-17.1,-16.0)$ mas yr^{-1}, while the NPM gives $(-7.8,-9.0)$, in fair agreement; I again adopt the MDM measurement because of its small formal error.

The measurement is $\pi_{\rm abs}=8.9\pm1.7$ mas, or 112 pc at face value. The magnitude constraint peaks around 6 mas, and the proper motion probability density peaks at just less than 3 mas (and the smaller NPM proper motion would push it still farther away). The Bayesian distance estimate is 160 (+65, −37) pc; the parallax contributes significantly to bring the distance closer than the small proper motion would suggest.

YZ Cnc: The parallax measurement is barely significant at 4.4 ± 1.7 mas. The MDM proper motion, (+23.9, −47.7) mas yr^{-1}, agrees well with NPM, (+18.2, −48.8) mas yr^{-1}. The proper motion probability peaks near $\pi=8$ mas. The orbital period of this SU UMa-type star was determined to be 2.08 hr by Shafter & Hessman (1988), who argue that the orbital inclination is around 40 deg. From this we estimate $M_V({\rm max})=4.6\pm3.0$, and for normal outbursts we take $V=12.0$ from Patterson (1979). The prior probability density based on the magnitudes peaks just above $\pi=3$ mas. The final Bayesian distance estimate is 256 (−70,+220) pc. The Bayesian probability density is double-peaked, evidently an artifact of the low-weight, high-velocity tail on the assumed velocity distribution, which extends some likelihood into the region where π^{-4} increases rapidly as π decreases. Interestingly, Dhillon et al. (2000) did not detect a secondary in the infrared and from this deduced $d>290$ pc if the secondary's spectral type is as expected. The present result is consistent with this limit. However, if the higher-velocity component of the velocity distribution is removed, the upper distance limit is sharply curtailed, and the Bayesian estimate becomes 222 (+50,−42) pc. In this case the rapidly falling probability densities of the proper motion and parallax combine to cut off the long-distance end.

While this paper was in the final stages of preparation, I became aware of an HST FGS parallax of YZ Cnc: Harrison et al. (2003a), find $\pi_{\rm abs}=3.34\pm0.45$ mas, and derive a Lutz-Kelker corrected value near 3.1 mas, for a distance near 320 ± 40 pc. The present result is at least nicely consistent with this much more precise value.

GP Com: The distance is well-constrained by $\pi_{\rm abs}=14.8\pm1.3$ mas. Because GP Com is an unusual double-degenerate helium CV (Marsh 1999), the absolute magnitude constraint was relaxed to $M_V=10\pm8$, unweighting it almost completely in the distance estimate. The proper motion is large – $(-337,+48)$ mas yr^{-1} in the present study, and $(-343,+32)$ mas yr^{-1} in NPM, so the transverse velocity $v_T=110$ km s^{-1} at $d=1/\pi_{\rm abs}$. This places GP Com on the outer limits of the core velocity distribution, but comfortably within the higher-velocity component. The low-velocity component of the proper motion distribution still carries some weight at 100 km s^{-1}, and it pulls the Bayesian distance estimate closer than $1/\pi_{\rm abs}$, almost perfectly canceling the Lutz-Kelker bias. The final Bayesian distance estimate is $68(+7,-6)$ pc.

EF Eri: Due to the faintness of this star, which was in its low state for all the parallax

observations, the fit residuals for single observations are relatively large (15 mas on average). This and the relatively sparse reference frame yielded a fairly uncertain parallax, $\pi_{\rm abs} = 5.5 \pm 2.5$ mas, so the Bayesian priors have a substantial effect. The MDM proper motion (which we adopt) is quite large, (+118.9, −44.5) mas yr^{-1}, with a formal error of 0.8 mas yr^{-1}; it disagrees significantly with the still larger NPM motion, (+144.2, −55.1) mas yr^{-1}. The best photometric constraint comes from Beuermann et al. (2000), who studied the low-state spectrum and identified the white dwarf contribution. For $M_{\rm wd} = 0.7$ M$_\odot$, they estimate $d = 110$ pc. We therefore form the constraint by adjusting m and M to yield $m - M = 5.2 \pm 1.0$. At $d = 1/\pi_{\rm abs}$, $v_T = 95$ km s^{-1}, so the assumed high-velocity component in the population is important, giving a final distance estimate of $d = 163(+66, -50)$ pc. Both the proper motion and magnitude priors push the estimate to lower distances than the parallax, and again the Bayesian median distance is slightly more nearby than $1/\pi_{\rm abs}$ despite the Lutz-Kelker bias. As in the case of YZ Cnc, the Bayesian result depends critically on including a high-velocity population in the velocity prior; removing the small admixture of high-velocity stars yields a considerably lower distance, $113(+19, -16)$ pc. The formal uncertainty is relatively small in this instance because the best compromise value lies far from the peaks of both the parallax and proper motion probability densities, so the net probability drops away quickly on each side of its maximum. All told, the parallax does tend to push the distance well out beyond what one would guess from the proper motion alone, and a little farther than the white-dwarf atmospheres argument would suggest.

AH Her: A parallax is barely detected, $\pi_{\rm abs} = 3.0 \pm 1.5$ mas. The MDM proper motion is very small, (0.0, +9.3) mas yr^{-1}, in excellent agreement with NPM which gives (−0.8, +10.8). Bruch (1987) thoroughly studied the distance constraint from the secondary star and concluded that the most likely distance was 350 to 500 pc, the spectral type of the secondary being the biggest contributor to the uncertainty. The Warner (1987) relation gives a very similar distance, using $i = 46 \pm 3$ deg from Horne, Wade, & Szkody (1986), and $V_{\rm max} = 11.6$ from Spogli et al. (2002). For the magnitude prior I therefore adopt $m - M = 8.1 \pm 1.0$, equivalent to 416 pc = 1/2.4 mas. The proper motion probability density peaks at an even greater distance, though its median is around 370 pc. Because of the large relative parallax error, and the small proper motion, this object is heavily influenced by the π^{-4} effect, and the Bayesian distance estimate is $d = 660(+270, -200)$ pc.

AM Her: The parallax, $\pi_{\rm abs} = 13.0 \pm 1.1$ mas, is accurate enough to dominate the distance estimate. The MDM proper motion is very substantial at (−39.9, +29.7) mas yr^{-1}; it agrees well with the USNO B1.0 (Monet et al. 2003), which lists (−41, +28). Young & Schneider (1981) detected the M4+V secondary and estimated $d = 71 \pm 18$ pc for a radius typical of the main sequence; for a somewhat larger secondary they estimated 93 pc. From this we adopt $m - M = 4.5 \pm 1.5$ for the magnitude prior, which gives a probability peak almost identical to $\pi_{\rm abs}$. The proper motion probability density peaks near $\pi = 9$ mas, and the final distance estimate is $79(+8, -7)$ pc, just slightly farther than $1/\pi_{\rm abs}$. The parallax adds weight and precision to previous estimates, but does not revise them significantly.

T Leo: The parallax, $\pi_{\rm abs} = 10.2 \pm 1.2$, yields $d = 98$ pc, and is accurate enough to dominate the distance determination. The large MDM proper motion, $(-86.3, -50.2)$ mas yr^{-1}, compares with $(-87.9, -66.1)$ in the NPM, and gives a probability density peaking around 70 pc. Shafter & Szkody (1984) measured the 84.7 min orbital period, and estimated $28 \leq i \leq 65$ deg, from which the Warner (1987) relations yield $4.6 \leq M_{V(\rm max)} \leq 6.2$; to be conservative I take $M_{V(\rm max)} = 5.4 \pm 3.0$. At supermaximum this SU UMa star reaches around $V = 10.0$ (Howell et al. 1999; Kato 1997), so I adopt $V = 11$ for ordinary maxima, yielding a most probable distance of 132 pc from the magnitude constraint alone. The final Bayesian distance estimate is 101 $(+13, -11)$ pc. Dhillon et al. (2000) use their non-detection of the secondary star in the infrared to establish $d > 120$ pc; the parallax argues for a distance near their lower limit, and suggests that the secondary lurks just below their sensitivity.

GW Lib: GW Lib's orbital period, $P_{\rm orb} = 76.8$ min, is the shortest known among dwarf novae with normal-composition secondaries (Thorstensen et al. 2002). The parallax, $\pi_{\rm abs} = 11.5 \pm 2.4$, is not particularly accurate. The MDM proper motion, $(-62, +28)$ mas yr^{-1} is quite substantial, and agrees fairly well with $(-58, +20)$ listed in USNO B1.0. This dwarf nova has only been seen in outburst once, and it was poorly observed; Thorstensen et al. (2002) estimated $d = 125$ pc from the available outburst information. The white dwarf is visible in the spectrum. Szkody et al. (2002b) fit $\log g = 8$ models of white dwarf atmosphere to HST ultraviolet data, and found distances of 171 and 148 pc depending on the temperatures used, but did not constrain $\log g$ independently and did not explore the distance parameter space. For the present study the absolute magnitude prior was set arbitrarily to $m - M = +5.5 \pm 3$ to match the (poorly determined) outburst absolute magnitude, effectively unweighting this constraint. The sizable relative parallax error creates a substantial Bayes-Lutz correction, but the large proper motion counteracts this, leading to a final distance estimate of $104(+30, -20)$ pc.

V893 Sco: This relatively bright dwarf nova had been lost until its identification was clarified by Kato et al. (1998). This field is sparsely observed, yielding $\pi_{\rm abs} = 7.4 \pm 2.4$ mas. The MDM proper motion is $(-53, -53)$ mas yr^{-1}. The period is 1.823 hr, and the inclination is constrained by eclipses (Bruch, Steiner, & Gneiding 2000), leading to an estimated M_V at maximum of 6.0 ± 2.0 (we adopt 2 mag rather than 3 mag for the uncertainty because of the quality of the inclination constraint), and Kato, Matsumoto, & Uemura (2002) find that normal outbursts reach $V = 12.5$; the probability density from this constraint peaks around $\pi = 5$ mas. The proper motion probability density peaks around 11 mas. The final distance estimate is $155(+58, -34)$ pc.

WZ Sge: This is the best-determined parallax in this study, $\pi_{\rm abs} = 23.2 \pm 0.8$ mas.

The parallax is accurate enough that the Bayesian priors have almost no effect, but the absolute magnitude estimate will be used later, so details are given here. All of WZ Sge's outbursts are superoutbursts, and they reach $V = 8.2$ (Patterson et al. 2002), which would imply a normal outburst magnitude of $V = 9.2$, if normal outbursts actually occurred. Spruit & Rutten (1998) find $i = 77 \pm 2$ degrees, and I double this uncertainty to be conservative. The inclination-adjusted

M_V-$P_{\rm orb}$ relation then implies $M_V = 6.7$. For the Bayesian estimate an uncertainty of 3 mag was assumed, effectively unweighting this constraint. The MDM proper motion is $(+74.3, -19.5)$ mas yr^{-1}, leading to a proper motion probability density peaking at $\pi = 15$ mas. The final distance estimate is $43.3(+1.6, -1.5)$ pc.

The literature contains many other estimates for the distance of WZ Sge. Smak (1993) estimated 48 ± 10 pc from the flux of the white dwarf, for which he adopts $M_{\rm wd} = 0.45 M_\odot$. Sion et al. (1995) model an HST ultraviolet spectrum with a $\log g = 8$ white dwarf, and find 69 pc for the distance. However, Spruit & Rutten (1998) point out that the temperature and gravity are highly degenerate in this kind of fit; largely from a study of the stream dynamics they adopt $\log g = 9$ for the white dwarf, and argue that the Sion et al. (1995) distance should be adjusted downward to 48 pc. The short distance determined here supports their interpretation, and suggests that the white dwarf in WZ Sge is relatively high-gravity (hence massive). WZ Sge is evidently the closest known cataclysmic binary.

While this paper was in the final stages of preparation, two other measurements of the parallax of WZ Sge came to my attention. First, C. Dahn (private communication) kindly passed along a USNO $\pi_{\rm rel}$ for WZ Sge closely agreeing with the present determination. Second, Harrison et al. (2003a) announced an even more precise $\pi_{\rm abs} = 22.97 \pm 0.15$ mas from the the HST Fine Guidance System, which also agrees accurately with this one. With three independent determinations giving essentially the same value, we can be very confident about the distance to WZ Sge.

SU UMa: The proper is small, $(+2, -16)$ mas yr^{-1}, which compares with $(+11.2, -25.2)$ mas yr^{-1} in the Lick NPM. The photometric constraint is based on $V = +12.0$ for normal outbursts (Rosenzweig et al. 2000), and the Warner relation with an ill-constrained binary inclination of 60 degrees, based on the modest velocity amplitude (Thorstensen, Wade, & Oke 1986). The parallax, $\pi_{\rm abs} = 7.4$ mas, is not well-determined, and the distance estimate depends critically on the error estimate adopted; the scatter about the best fit indicates $\sigma = 1.4$ mas, while the scatter of six comparison stars within 2 mag of SU UMa gives 2.4 mas. Adopting the smaller error yields a Bayesian estimate of 189 $(+79, -43)$ pc; if the larger error is adopted, the Lutz-Kelker correction increases the estimate to 403 $(+230, -162)$ pc. While the distance is disappointingly indeterminate, 120 pc is a reasonable lower limit.

HV Vir: This star resembles WZ Sge in that it outbursts only rarely and with large amplitude. Because of its faintness, the parallax is somewhat uncertain at $\pi_{\rm abs} = 5.8 \pm 2.2$ mas. The proper motion is modest, $(+19, -12)$ mas yr^{-1}. in good agreement with $(+22, -8)$ in USNO B1.0. The superoutburst light curve (Leibowitz et al. 1994) reaches $V = 11.5$, indicating that if normal outbursts occurred (which they apparently don't), they would reach ~ 12.5. The orbital period, from low-state photometry, is 0.05799 d, and the presence of a low-state modulation suggests a substantial orbital inclination, yielding an estimated $M_V = 5.9 \pm 3$. The resulting photometric constraint peaks near $\pi = 5$ mas. The small proper motion puts the star more distant, with a peak near $\pi = 3$ mas. The rather weak parallax determination leads to a substantial π^{-4} effect, and

a final Bayesian distance estimate of 460 $(+530, -180)$ pc. For comparison, Szkody et al. (2002a) estimate a distance in the 400 – 550 pc range from the white dwarf's UV continuum. WZ Sge is about 4.5 mag brighter than HV Vir; assuming they are identical yields a distance estimate near 350 pc, in reasonable agreement with the Bayesian estimate.

6. Discussion

Although the distance scale for cataclysmics has been uncertain (as noted in the Introduction), over the years some 'conventional wisdom' has grown up around cataclysmic distances, based on detections of secondary stars, kinematical evidence, and the like. How well does the conventional wisdom bear up?

Dwarf Novae. We can use the dwarf novae for which we have usable distance estimates to test the M_V(max-$P_{\rm orb}$ correlation (Warner 1987, 1995). Table 5 and Fig. 3 show this test[6]. There are several complications, as follows: (1) Warner's correlation depends on a correction for orbital inclination, which is often poorly known; the text of the previous section gives the evidence used to constrain i. The values of M_V (pred) in Table 5 and Fig. 3 are for the assumed inclination, rather than corrected to a particular fiducial inclination, so they should be directly comparable to observation. The error bars on the predicted M_V reflect only the uncertainty in the inclination, and *ignore* any 'cosmic scatter' in the relation. (2) The superoutbursts of SU UMa stars are about one magnitude brighter than the normal outbursts. For those SU UMa stars for which I was unable to find literature references to $V_{\rm max}$ for normal outbursts I've added 1 mag to the superoutburst maximum. In the WZ Sge, HV Vir, and GW Lib, normal outbursts are not observed, but the same correction was adopted.

In view of the crude assumptions – especially the arbitrary 1-magnitude correction between normal and superoutbursts, and the unreliability of some of the inclinations – the agreement appears to be satisfactory. Although the data appear too sparse to uncover the relationship independently, none of the stars are markedly discrepant. The rarely-outbursting, large-amplitude objects – WZ Sge, HV Vir, and GW Lib – do not disagree dramatically with expectations. Even so, WZ Sge is measured to be somewhat farther away than one would predict on the basis of the relation, which is puzzling in that it has an accurate magnitude, a well-constrained inclination, and a very accurately-determined distance. Adopting the actual superoutburst $V_{\rm max}$ for the maximum magnitude would make the discrepancy worse. It is possible that the disk in WZ Sge expands to be unusually large during its outbursts, increasing its intrinsic brightness beyond expectation, or that the expression used by Warner for the inclination correction becomes inaccurate at high inclinations. SS Aur is also slightly discrepant (less than two standard deviations), in the sense that the predicted

[6]In order to avoid circular arguments the distance estimates employed in this comparison are based on the parallax and proper motion only, without the magnitude constraint.

absolute magnitude is fainter than the empirical one. The inclination is not strongly constrained, but is already assumed to be fairly modest, and even adopting a face-on inclination would not brighten the predicted magnitude appreciably. However, the more accurate HST FGS parallax (Harrison et al. 2000) brings the empirical absolute magnitude to 3.8, much closer to the predicted value.

Harrison et al. (2003a) discuss the M_V (max) - $P_{\rm orb}$ relation at greater length using the HST parallaxes, and confirm that the relationship appears to hold.

AM Her stars. The parallax of AM Her agrees well with distances based on the spectrum of the secondary. EF Eri is not accurately determined but comes in a little farther away than the white dwarf atmosphere (Beuermann et al. 2000) would suggest. Harrison et al. (2003) have recently measured and modeled infrared spectra and light curves of EF Eri, but do not comment on how the models are normalized to the data (that is, the distance); the infrared light curve is quite complicated and so model dependencies are likely to creep into such determinations in any case.

Helium CVs. GP Com was the only helium CV included, but it appears to be the first to have an accurate distance determination. Taking our measured $V = 16.1$ as typical, the measured distance modulus $m - M = 4.2 \pm 0.2$ yields $M_V = +11.9$.

7. Conclusions

The main conclusions are as follows.

(1) As USNO92 assert, interestingly accurate parallaxes can be derived without special equipment, provided the instrumentation is stable.

(2) Over the years a fair amount of conventional wisdom has grown up around cataclysmic distances, based on detections of secondary stars, kinematical evidence, and the like. This study largely corroborates this conventional wisdom; a one-line summary might be 'no big surprises'.

(3) Even so, there are some small surprises. WZ Sge is a little closer than some previous estimates had suggested, and a little farther away than predicted by the M_V(max) - $P_{\rm orb}$ relation. Although the result for EF Eri is imprecise, it appears to be a little farther away than anticipated.

(4) GP Com is evidently the first helium CV with a reliable distance. It is intrinsically faint ($M_V = +11.9$). Furthermore, its transverse velocity is 110 km s^{-1}, outside the rather small velocity dispersion of the main CV population.

Acknowledgments. Special thanks go to Dave Monet for encouragement and free advice, which was infinitely many times more valuable than its price, and for his role in pioneering this powerful technique. Conard Dahn communicated a USNO parallax for WZ Sge while this paper was in preparation, and it was a great confidence-builder to find it was essentially identical to that pre-

sented here. Also, Tom Harrison kindly communicated the wonderfully accurate HST parallaxes just as I was completing this paper. Tom Marsh suggested GP Com as a target. After I had begun development of the Bayesian distance estimation techniques I discovered that Haywood Smith had already explored this approach thoroughly, and he offered much thoughtful advice. Graduate students Cindy Taylor and Bill Fenton took data on several observing runs. The MDM staff and director put up with extra instrument changes so that this program could be shoehorned into time otherwise used for spectroscopy. Joe Patterson made some thoughtful comments. Last but not least, I thank the NSF (AST 9987334 and AST 0307413) for support.

REFERENCES

Bailey, J. 1981, MNRAS, 197, 31

Berriman, G. 1987, A&AS, 68, 41

Berriman, G., Szkody, P., & Capps, R. W. 1985, MNRAS, 217, 327

Bertin, E. & Arnouts, S. 1996, A&AS, 117, 393

Bessell, M. S. 1990, PASP, 102, 1181

Beuermann, K., Baraffe, I., & Hauschildt, P. 1999, A&A, 348, 524

Beuermann, K., Wheatley, P., Ramsay, G., Euchner, F., & Gänsicke, B. T. 2000, A&A, 354, L49

Bruch, A. 1987, A&A, 172, 187

Bruch, A., Steiner, J. E., & Gneiding, C. D. 2000, PASP, 112, 237

Cash, W. 1979, ApJ, 228, 939

Dahn, C. C. et al. 2002, AJ, 124, 1170

Dhillon, V. S., Littlefair, S. P., Howell, S. B., Ciardi, D. R., Harrop-Allin, M. K., and Marsh, T. R. 2000, MNRAS, 314, 826

Duerbeck, H. W. 1999, Informational Bulletin on Variable Stars, 4731, 1

Friend, M. T., Martin, J. S., Smith, R. C., and Jones, D. H. P. 1990, MNRAS, 246, 637

Gubler, J. & Tytler, D. 1998, PASP, 110, 738

Harrison, T. E., McNamara, B. J., Szkody, P., McArthur, B. E., Benedict, G. F., Klemola, A. R., & Gilliland, R. L. 1999, ApJ, 515, L93

Harrison, T. E., McNamara, B. J., Szkody, P., & Gilliland, R. L. 2000, AJ, 120, 2649

Harrison, T. E., Howell, S. B., Huber, M. E., Osborne, H. L., Holtzman, J. A., Cash, J. L., & Gelino, D. M. 2003, AJ, 125, 2609

Harrison, T. E., Johnson, J. J., McArthur, B. E., Benedict, G. F., Szkody, P., Howell, S. B., & Gelino, D. M. 2003, AJ, in preparation.

Horne, K., Wade, R. A., & Szkody, P. 1986, MNRAS, 219, 791

Howell, S. B., Ciardi, D. R., Szkody, P., van Paradijs, J., Kuulkers, E., Cash, J., Sirk, M., & Long, K. S. 1999, PASP, 111, 342

Kamper, K. W. 1979, IAU Colloq. 53: White Dwarfs and Variable Degenerate Stars, 494

Kato, T. 1997, PASJ, 49, 583

Kato, T., Haseda, K., Takamizawa, K., Kazarovets, E. V., & Samus, N. N. 1998, Informational Bulletin on Variable Stars, 4585, 1

Kato, T., Matsumoto, K., & Uemura, M. 2002, Informational Bulletin on Variable Stars, 5262, 1

Klemola, A. R., Jones, B. F., & Hanson, R. B. 1987, AJ, 94, 501

Kolb, U. & Stehle, R. 1996, MNRAS, 282, 1454

Kraft, R. P. & Luyten, W. J. 1965, ApJ, 142, 1041

Kraft, R. P., Krzeminski, W., and Mumford, G. S. 1969, ApJ, 158, 589

Landolt, A. U. 1992, AJ, 104, 340

Leibowitz, E. M., Mendelson, H., Bruch, A., Duerbeck, H. W., & Seitter, W. C. 1994, ApJ, 421, 771

Loredo, T. J. 1992, in Feigelson, E. D., & Babu, G. J. (ed.) Statistical Challenges in Modern Astronomy, New York:Springer Verlag, p. 275

Lutz, T. E. & Kelker, D. H. 1973, PASP, 85, 573

Marsh, T. R. 1999, MNRAS, 304, 443

McArthur, B. E. et al. 1999, ApJ, 520, L59

McArthur, B. E. et al. 2001, ApJ, 560, 907

Mennickent, R. E., and Diaz, M. P. 2002, MNRAS, 336, 767

Mihalas, D., & Binney, J., Galactic Astronomy, 2nd ed., (Freeman:San Francisco)

Monet, D. G. & Dahn, C. C. 1983, AJ, 88, 1489

Monet, D. G., Dahn, C. C., Vrba, F. J., Harris, H. C., Pier, J. R., Luginbuhl, C. B., & Ables, H. D. 1992, AJ, 103, 638 (USNO92)

Monet, D. et al. 1996, USNO-A2.0, (U. S. Naval Observatory, Washington, DC)

Monet, D. G. et al. 2003, AJ, 125, 984

North, R. C., Marsh, T. R., Kolb, U., Dhillon, V. S., & Moran, C. K. J. 2002, MNRAS, 337, 1215

Oppenheimer, B. D., Kenyon, S. J., & Mattei, J. A. 1998, AJ, 115, 1175

Patterson, J. 1979, AJ, 84, 804

Patterson, J., Bond, H. E., Grauer, A. D., Shafter, A. W., & Mattei, J. A. 1993, PASP, 105, 69

Patterson, J. et al. 2002, PASP, 114, 721

Pickles, A. J. 1998, PASP, 110, 863

Rosenzweig, P., Mattei, J. A., Kafka, S., Turner, G. W., & Honeycutt, R. K. 2000, PASP, 112, 632

Shafter, A. M., and Szkody, P. 1984, ApJ, 276, 305

Shafter, A. W., and Hessman, F. V. 1988, AJ, 95, 178

Sion, E. M., Cheng, F. H., Long, K. S., Szkody, P., Gilliland, R. L., Huang, M., & Hubeny, I. 1995, ApJ, 439, 957

Smak, J. 1993, Acta Astronomica, 43, 101

Smith, H. 1987, A&A, 171, 336

Smith, H. 1987, A&A, 171, 342

Spogli, C., Fiorucci, M., Tosti, G., Ciprini, S., Nucciarelli, G., Macchia, E., and Monacelli, G. 2002, IBVS No. 5276

Sproats, L. N., Howell, S. B., & Mason, K. O. 1996, MNRAS, 282, 1211

Spruit, H. C. & Rutten, R. G. M. 1998, MNRAS, 299, 768

Stetson, P. B. 1987, PASP, 99, 191

Szkody, P., Gaensicke, B. T., Sion, E. M., and Howell, S. B. 2002, ApJ, 574, 950

Szkody, P., Gänsicke, B. T., Howell, S. B., & Sion, E. M. 2002, ApJ, 575, L79

Szkody, P., and Wade, R. A. 1981, ApJ, 251, 201

Thorstensen, J. R, and Ringwald, F. A. 1995, IBVS, No. 4249

Thorstensen, J. R., Patterson, J., Thomas, G., & Shambrook, A. 1996, PASP, 108, 73

Thorstensen, J. R. 1997, PASP, 109, 1241

Thorstensen, J. R., & Taylor, C. J. 1997, PASP, 109, 1359

Thorstensen, J. R., Patterson, J., Kemp, J., & Vennes, S. 2002, PASP, 114, 1108

Thorstensen, J. R., & Fenton, W. H. 2003, PASP, 115, 37

Thorstensen, J. R., & Kirkpatrick, J. D. 2003, PASP, in press.

Thorstensen, J. R., Wade, R. A., and Oke, J. B. 1986, ApJ, 309, 721

van Paradijs, J., Augusteijn, T., & Stehle, R. 1996, A&A, 312, 93

Wallace, P. T. 1994, ASP Conf. Ser. 61: Astronomical Data Analysis Software and Systems III, 3, 481

Warner, B. 1987, MNRAS, 227, 23

Warner, B. 1995, Cataclysmic Variables (Cambridge University Press)

Young, P., and Schneider, D. P. 1981, ApJ, 247, 960

Table 1. Journal of Observations

Star	$N_{\rm ref}$	$N_{\rm meas}$	$N_{\rm pix}$	Epochs
VY Aqr	15	22	139	1997.71(17) , 1997.95(5) , 1998.44(8) , 1998.69(11) , 1999.43(21) , 1999.79(27) , 2000.50(24) , 2002.81(8) , 2003.46(18)
SS Aur	59	148	132	1997.71(9) , 1997.96(15) , 1999.05(44) , 1999.79(37) , 2000.03(15) , 2000.26(6) , 2002.05(6)
Z Cam	11	32	59	1997.95(19) , 1998.21(6) , 1999.05(19) , 1999.79(11) , 2000.03(4)
YZ Cnc	25	50	83	1997.95(5) , 1998.21(6) , 1999.05(18) , 1999.79(5) , 2000.03(9) , 2000.26(30) , 2002.05(10)
GP Com	13	31	152	1999.43(19) , 2000.03(24) , 2000.26(23) , 2000.50(12) , 2001.24(20) , 2001.39(24) , 2003.08(17) , 2003.46(13)
EF Eri	13	28	105	1997.71(19) , 1997.95(7) , 1999.05(14) , 1999.79(9) , 2000.03(26) , 2002.05(11) , 2003.08(19)
AH Her	17	80	93	1998.21(17) , 1998.44(14) , 1998.69(3) , 1999.43(30) , 2000.26(7) , 2001.24(6) , 2001.39(16)
AM Her	24	54	105	1997.71(11) , 1998.21(19) , 1998.44(14) , 1998.69(5) , 1999.43(25) , 2000.26(19) , 2000.50(9) , 2001.39(3)
T Leo	15	24	130	1997.95(1) , 1998.21(12) , 1998.44(6) , 1999.05(7) , 1999.43(11) , 2000.03(41) , 2000.26(18) , 2001.24(4) , 2002.05(13) , 2003.08(17)
GW Lib	41	110	70	2000.26(19) , 2000.50(15) , 2001.24(9) , 2001.39(19) , 2001.46(2) , 2003.08(6)
V893 Sco	47	187	83	2000.26(22) , 2000.50(21) , 2001.24(10) , 2001.39(13) , 2003.46(17)
WZ Sge	45	77	162	1997.71(12) , 1998.44(15) , 1999.43(44) , 1999.79(15) , 2000.50(36) , 2001.39(21) , 2002.81(19)
SU UMa	10	25	90	1997.96(17) , 1998.21(2) , 1999.05(14) , 1999.79(2) , 2000.03(30) , 2000.26(9) , 2002.05(9) , 2003.08(7)
HV Vir	12	32	111	1998.21(13) , 1998.44(10) , 1999.05(29) , 1999.43(29) , 2000.26(20) , 2001.24(4) , 2001.39(6)
LHS429	17	41	58	1998.21(4), 1998.44(8), 1999.43(15), 2000.26(6), 2000.50(5), 2001.39(20)
LHS483	40	84	62	1997.71(6), 1998.44(5), 1999.43(7), 1999.79(3), 2000.50(11), 2001.39(20), 2002.81(10)
LHS1801+2	25	59	65	1997.71(14), 1998.21(6), 1999.04(21), 1999.79(9), 2000.03(5), 2002.05(10)
LHS1889	46	68	63	1999.05(29), 1999.79(8), 2000.03(8), 2001.24(10), 2002.81(8)
LHS3974	22	51	63	1997.71(14), 1997.96(16), 1998.68(5), 1999.79(22), 2002.81(6)

Note. — Overview of the data included in the parallax solutions. $N_{\rm ref}$ is the number of reference stars used to define the plate solution, $N_{\rm meas}$ is the total number of stars measured, and $N_{\rm pix}$ is the number of images used. The epochs represent different observing runs, and the numbers in parentheses are the number of images included from each run.

Table 2. Positions, Magnitudes, Parallaxes, and Proper Motions

α [J2000]	δ [J2000]	Weight	σ [mas]	V	$V-I$	$\pi_{\rm rel}$ [mas]	μ_X [mas y^{-1}]	μ_Y [mas y^{-1}]	σ_μ [mas y^{-1}]
				VY Aqr:					
21:12:05.70	-8:47:48.5	0	17	17.97	0.90	-0.3 ± 1.9	-6.6	-2.8	0.8
21:12:08.65	-8:47:47.0	1	8	15.18	0.97	1.1 ± 0.8	0.2	7.6	0.4
21:12:09.90	-8:47:53.1	1	8	17.27	1.05	1.3 ± 0.9	-10.3	0.9	0.4
21:11:56.61	-8:48:05.7	1	9	16.36	1.00	-1.5 ± 1.0	5.4	-4.4	0.4
21:12:17.21	-8:47:56.6	1	9	17.32	1.28	-0.6 ± 0.9	6.4	-1.9	0.4
21:12:13.26	-8:48:14.6	1	10	16.98	1.04	-1.3 ± 1.1	0.3	-17.3	0.5

Note. — Parameters for all measured stars in all the fields. Program stars are marked with an asterisk. The fourth star listed in the LHS 1889 field proved to be a hitherto unknown L3.5 dwarf. The celestial coordinates are from mean CCD images and are referred to the USNO A2.0, which is in turn aligned with the ICRS; the epochs of the images used are typically around 1998. Coordinates should be accurate to $\sim 0''.3$ external and somewhat better than this internally. A 1 or 0 in the next column indicates whether a star was used as a reference star. The next column gives the scatter around the best astrometric fit (see text); in a few cases these are very large (e.g. close pairs which were intermittently resolved). The V and $V-I$ colors come next, with typical external uncertainties of 0.05 mag and internal consistency somewhat better than that. Next come the fitted parallaxes, proper motions in X and Y, and the uncertainty in the proper motion (per coordinate). Full table available in the electronic version of this paper.

Table 3. LHS Stars Re-Observed

Star	Program	$\pi_{\rm rel}$ (mas)	$\mu_{X\,({\rm rel})}$ (mas yr^{-1})	$\mu_{Y\,({\rm rel})}$ (mas yr^{-1})	V	$V-I$
LHS429	USNO	153.9(0.7)	−814.7(0.6)	−869.1(0.6)	16.85	4.54
	MDM	154.5(2.4)	−811.5(1.0)	−865.5(0.9)	16.80	4.63
LHS483	USNO	56.7(0.8)	1066.1(0.4)	−78.5(0.4)	17.00	1.15
	MDM	58.8(1.2)	1059.6(0.8)	−78.9(0.8)	17.15	1.17
LHS1801	USNO	31.8(1.5)	13.9(1.0)	−532.7(1.0)	17.21	0.93
	MDM	30.6(1.6)	11.9(0.9)	−528.1(0.9)	17.20	0.95
LHS1802	USNO	36.4(1.1)	12.6(1.1)	−528.2(1.1)	15.46	2.86
	MDM	30.8(1.3)	11.4(0.7)	−524.8(0.7)	15.45	2.91
LHS1889	USNO	52.8(0.9)	358.7(0.6)	−578.4(0.6)	16.56	0.99
	MDM	49.6(1.5)	350.9(0.8)	−590.2(0.8)	16.57	1.00
LHS3974	USNO	13.2(0.7)	540.9(0.4)	19.3(0.4)	17.43	2.74
	MDM	11.8(1.3)	539.6(0.6)	17.0(0.6)	17.42	2.81

Table 4. Parallaxes, Proper Motions, and Distances

Star	$\pi_{\rm rel}$ $d_{\rm LK}$	$\pi_{\rm abs}$ $d(\pi,\mu)$	$[\mu_\alpha,\mu_\delta]_{\rm rel}$ $(m-M)$ prior	$1/\pi_{\rm abs}$ $d(\pi,\mu,m-M)$
VY Aqr	$10.2 \pm 1.4[1.1]$	11.2(1.4)	$+33.9, -38.4(0.8)$	$89(+13,-10)$
	96	$97(+15,-12)$	10.8; 5.8; 3.0	$97(+15,-12)$
SS Aur	$4.0 \pm 0.8[1.2]$	4.8(1.1)	$+1.7, -20.8(0.6)$	$208(+62,-39)$
	300	$300(+130,-75)$	12.66; 5.5; 1.0	$283(+90,-60)$
Z Cam	$7.7 \pm 1.8[1.3]$	8.9(1.7)	$-17.1, -16.0(2.0)$	$112(+27,-18)$
	137	$164(+88,-42)$	10.4; 4.3; 1.5	$163(+68,-38)$
YZ Cnc	$3.4 \pm 1.5[1.7]$	4.4(1.7)	$+23.9, -47.7(0.9)$	$230(+140,-60)$
	···	$260(+320,-70)$	12.0; 4.6; 3.0	$256(+290,-70)$
GP Com	$13.5 \pm 0.7[1.3]$	14.8(1.3)	$-336.8, +47.7(0.5)$	$69(+7,-6)$
	70	$68(+7,-6)$	15.7;10.0;8.0	$68(+7,-6)$
EF Eri	$3.9 \pm 1.6[2.5]$	5.5(2.5)	$+119, -45(0.8)$	$182(+152,-57)$
	···	$229(+85,-83)$	[5.2];1.0	$163(+66,-50)$
AH Her	$1.7 \pm 1.0[1.5]$	3(1.5)	$+0.0, +9.3(0.7)$	$330(+330,-110)$
	···	$1800(+2100,-900)$	[8.1]; 1.0	$660(+270,-200)$
AM Her	$12.0 \pm 1.0[1.1]$	13.0(1.1)	$-39.9, +29.7(0.9)$	$78(+7,-6)$
	79	$79(+8,-6)$	[4.5]; 1.5	$79(+8,-6)$
T Leo	$9.1 \pm 0.7[1.2]$	10.2(1.2)	$-86.3, -50.2(0.4)$	$98(+13,-10)$
	104	$101(+13.,-11)$	11.;5.4;3.	$101(+13,-11)$
GW Lib	$10.4 \pm 2.4[1.8]$	11.5(2.4)	$-61.5, +27.8(1.2)$	$87(+23,-15)$
	112	$104(+30,-20)$	9.0;3.5;3.0	$104(+30,-20)$
V893 Sco	$5.9 \pm 2.4[2.2]$	7.4(2.4)	$-52.6, -52.8(1.2)$	$135(+65,-33)$
	···	$153(+68,-35)$	12.5;6.0;2.0	$155(+58,-34)$
WZ Sge	$22.0 \pm 0.6[0.8]$	23.2(0.8)	$+74.3, -19.5(0.5)$	$43.1(+1.5,-1.4)$
	43.3	$43.3(+1.6,-1.5)$	9.2;6.7;3.0	$43.3(+1.6,-1.5)$

Table 4—Continued

Star	$\pi_{\rm rel}$ $d_{\rm LK}$	$\pi_{\rm abs}$ $d(\pi,\mu)$	$[\mu_\alpha,\mu_\delta]_{\rm rel}$ $(m-M)$ prior	$1/\pi_{\rm abs}$ $d(\pi,\mu,m-M)$
SU UMa	$6.6 \pm 1.4[1.7]$	7.4(1.7)	$+1.7, -16.1(1.5)$	$135(+40, -25)$
	194	$269(+240, -99)$	12.0;5.4;3.0	$260(+190, -90)$
HV Vir	$4.9 \pm 2.2[2.1]$	5.8(2.2)	$+19, -12(1.9)$	$172(+105, -47)$
	$\cdots$	$600(+1100, -280)$	$12.5; 5.9; 3.$	$460(+530, -180)$

Note. — Parallaxes (in mas), proper motions (in mas yr^{-1}), and distance estimates (in pc). Two lines are given for each star. In the first line, the uncertainties given for the relative parallaxes are derived from the goodness of fit, and the square-bracketed quantities are the uncertainties derived from the scatter of the reference stars (see text). The uncertainties in the proper motion do not take the uncertainty in the zero point into account, which is of order 5 mas yr^{-1} in most cases (see text). The last column gives the distance based on the absolute parallax alone with no corrections. The second line for each star lists the following: *Col 2.* The most probable value of the distance based on the absolute parallax and a Lutz-Kelker correction (i.e., Bayesian with minimal priors); no confidence interval is given because the cumulative distribution function is not normalizable in this case. *Col. 3* The Bayesian estimate considering the parallax and proper motion prior only. *Col. 4* The distance priors, expressed in magnitudes. Where three numbers are given they are the apparent magnitude, assumed absolute magnitude, and 1-sigma combined uncertainty (generally taken to be quite large to avoid undue circularity); where two numbers are given, they signify an assumed distance modulus $m - M$ and its associated uncertainty. In these cases, the distance prior is not associated with a literal apparent and absolute magnitude. *Col. 5* The Bayesian estimator taking into account parallax, proper motion, and the prior information from the previous column. In all these estimates, the errors quoted reflect the 16- and 84-percentile points in the cumulative distribution function.

Table 5. Measured and Theoretical Absolute Magnitudes

Star	$P_{\rm orb}$ (hr)	Inclination (deg)	$V_{\rm max}$	M_V(max) (pred)	M_V(max) (meas)
GW Lib	1.28	11 ± 10	10.0	$4.9(+0.5, -0.6)$	$4.4(+0.1, -0.0)$
WZ Sge	1.36	77 ± 5	9.2	$6.0(+0.1, -0.1)$	$6.7(+0.6, -0.4)$
HV Vir	1.39	60 ± 10	12.5	$3.6(+1.4, -2.3)$	$5.5(+0.6, -0.4)$
T Leo	1.42	47 ± 19	11.0	$6.0(+0.3, -0.3)$	$5.0(+0.8, -0.4)$
VY Aqr	1.51	63 ± 13	10.8	$5.9(+0.3, -0.3)$	$5.6(+0.9, -0.5)$
V893 Sco	1.82	71 ± 5	12.5	$6.6(+0.6, -0.8)$	$6.1(+0.4, -0.3)$
YZ Cnc	2.08	40 ± 10	12.0	$4.9(+0.7, -1.7)$	$4.7(+0.3, -0.2)$
SS Aur	4.39	39 ± 8	10.3	$2.9(+0.6, -0.8)$	$4.0(+0.2, -0.2)$
Z Cam	6.98	65 ± 10	10.4	$4.3(+0.6, -0.9)$	$4.3(+0.7, -0.5)$

Note. — The sources for the orbital inclinations and apparent V magnitude in *normal* outburst are given in the text. The predicted absolute magnitudes are computed from the relations given by Warner (1987) and Warner (1995), and the quoted uncertainties reflect *only* the uncertainty in the inclination. The absolute magnitudes at maximum light is computed from the apparent magnitude using the geometrically-based distance from Table 3 (excluding prior magnitude information). The uncertainty reflects only the uncertainty in distance; other less quantifiable uncertainties not taken into account include the appropriateness of the figure used for $V_{\rm max}$.

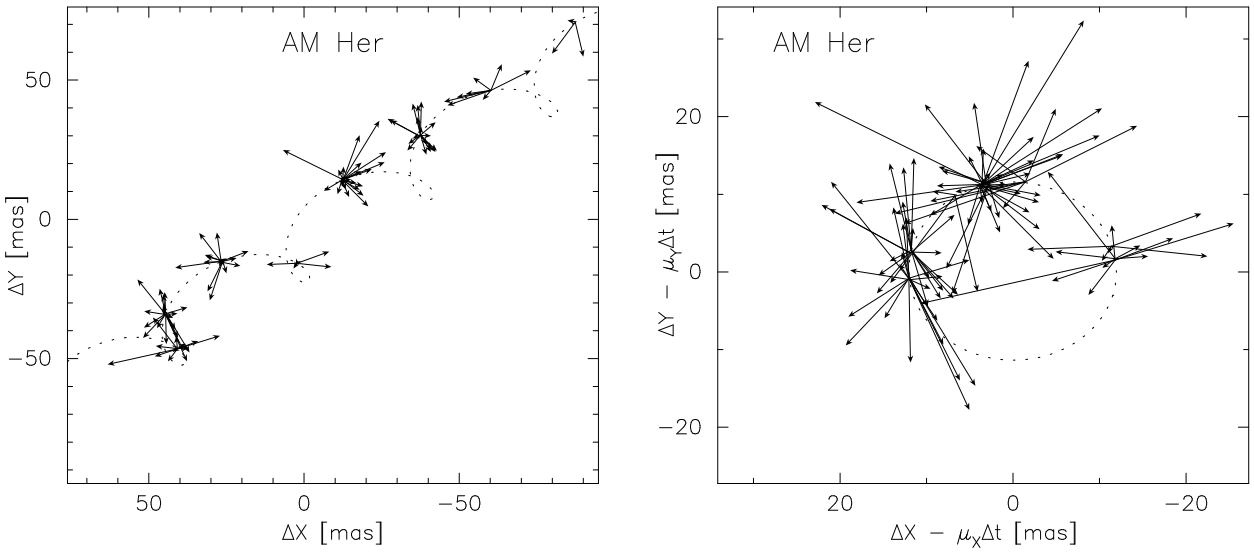

Fig. 1.— Fits to the positions of AM Her referred to its mean position. The tip of each arrow gives the position in a single image, and the tail is the position predicted by the fitted parallax, proper motion, and zero point. The left panel shows the trajectory across the sky, while the right panel shows the data and fit in a reference frame moving with the fitted proper motion, leaving only the parallax displacement. The parallactic ellipse is nearly circular because AM Her lies near the ecliptic pole.

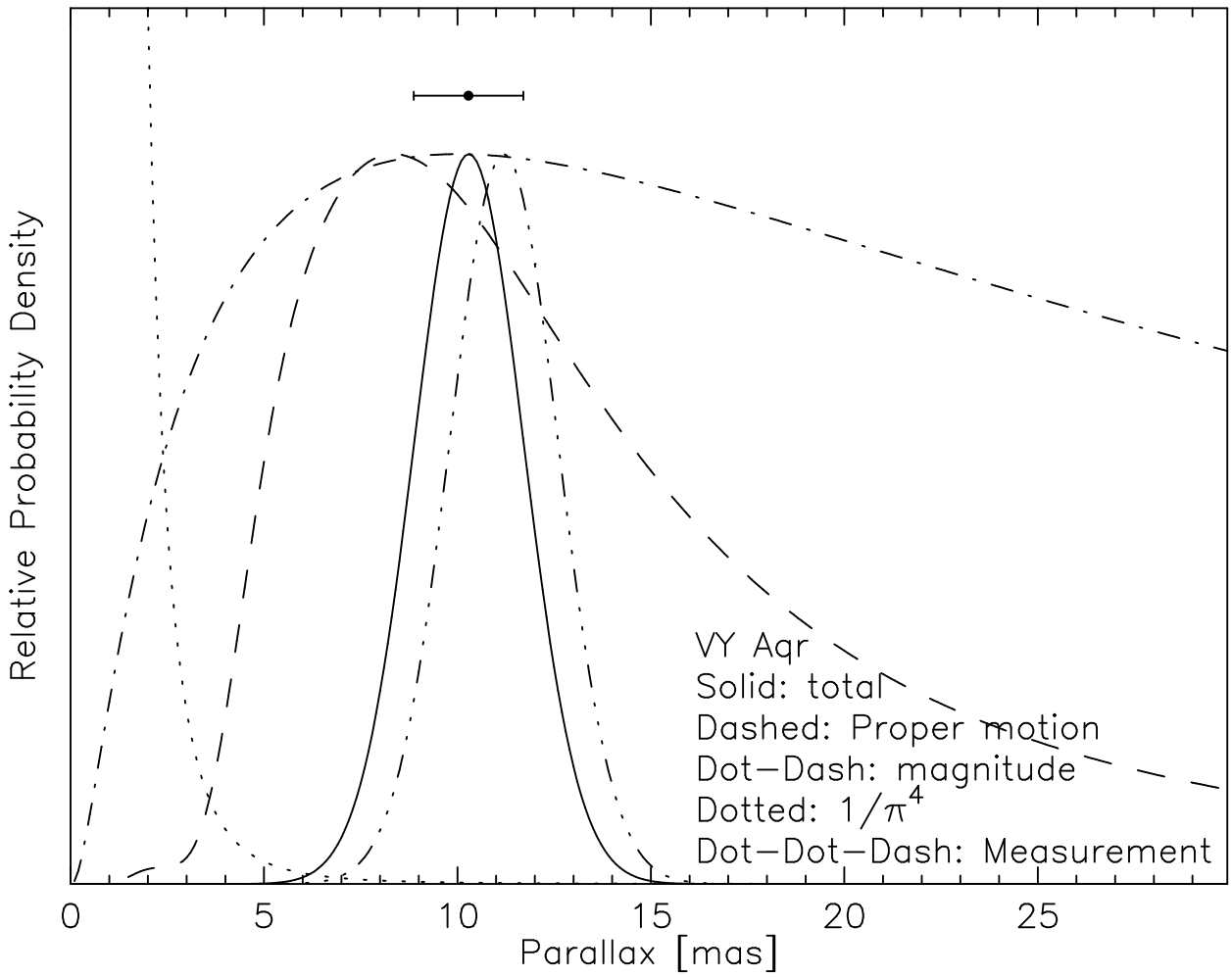

Fig. 2.— Illustration of the various contributions to the Bayesian distance-estimation procedure described in the text, for VY Aqr. The solid curve gives the net result, and the error bar above it gives the equivalent 1σ confidence interval. In this case the parallax measurement (dot-dot-dash curve) is precise enough that the other factors serve only to shift the result to slightly smaller parallaxes. The relative normalization of the various factors is arbitrary.

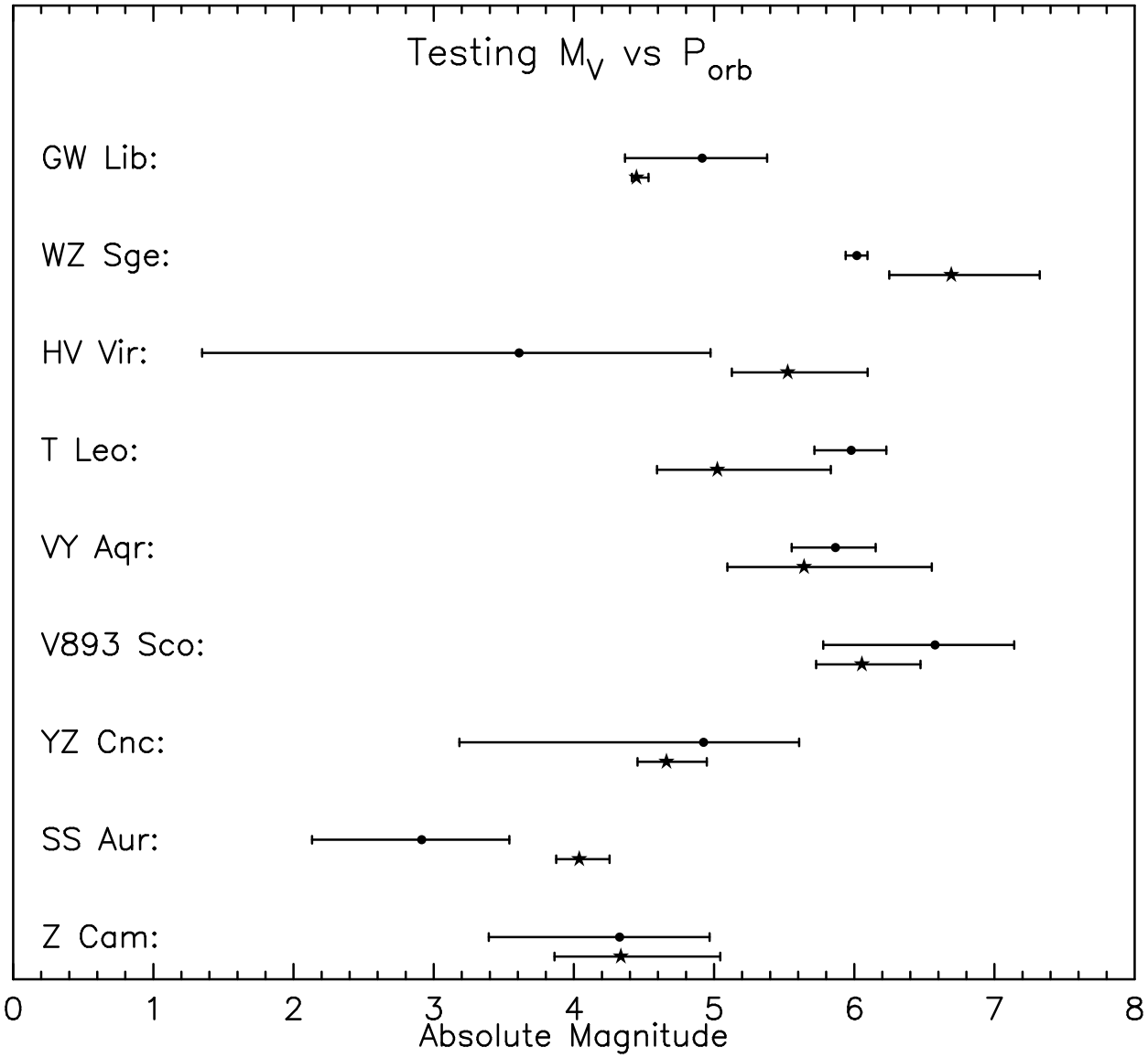

Fig. 3.— Graphical presentation of the empirical and predicted absolute V magnitude from Table 4. The stars are arranged in order of increasing period. The top error bar in each set (round dot) is the empirical value formed from the apparent V magnitude at maximum light and the distance inferred from the parallax and proper motion (only); the lower error bar (star) is the value predicted by the M_V (max) - $P_{\rm orb}$ relation. See the comments to Table 4.